https://erjm.journals.ekb.eg
ISSN: 1110-1180

DOI: ---------

ERJ
Engineering Research Journal
Faculty of Engineering
Menoufia University

Effects of Nanofluids on the Thermal Performance of Double Pipe Heat Exchanger

Samy M. El-Behery[1], Gamal H. Badawy[1], Wageeh A. El-Askary[1,2] and Fathi M. Mahfouz[1]

1 Mechanical Power Engineering Department, Faculty of Engineering, Menoufia University, Egypt.
2 Alexandria Higher Institute of Engineering and Technology (AIET), Egypt.

ABSTRACT
In the present study, the effect of nanofluids on the thermal performance of double pipe counter flow heat exchanger equipped with a decaying swirl flow system is numerically investigated. The swirl flow is generated using a tangential slot at the flow inlet of the outer pipe with a tangent angle of 30º. The volume concentrations of four different types of nanoparticles, Al_2O_3, CuO, TiO_2 and ZnO in the range of 0% to 3% and different nanoparticle diameters in the range of 20 nm to 50 nm are considered for each in this study. The results indicate that, the heat transfer coefficient and pressure drop increase with increasing Reynolds number and volume concentrations of nanofluids. All nanofluid types achieve better heat transfer enhancement compared to pure water with slight increases in the pressure drop. The Al_2O_3 nanomaterial has better thermal enhancement characteristics followed by CuO, ZnO, and TiO_2, respectively. The average heat transfer coefficient enhancement is 14% for the Al_2O_3 nanoparticles with a volume concentration of ϕ=3% and nanoparticle diameter of 32 nm, while the increase in pressure drop reaches 5% and 72% of pure water for the Al_2O_3 nanoparticles with a volume concentration of ϕ=0.5% and ϕ=3%, respectively. As the particle diameter decreases, the heat transfer as well as the effectiveness increase and there is a slight variation in the pressure drop. Finally, the use of nanofluids can be suggested as being effective method for enhancing the performance of heat exchanger.

Keywords: Nanofluids; Enhancement techniques; Double pipe heat exchanger; CFD simulation; Swirl flow.

1. Introduction

The heat exchanger is one of the most important devices in many practical applications. These applications include space heating, heat recovery, fluid heating in manufacturing, air conditioning, refrigeration, power plants, cogeneration plants, chemical and petrochemicals plants etc. In recent years, the development of heat exchangers performance has become necessary to energy saving. For several decades, the thermal and hydrodynamic characteristics evaluations associated with a heat exchanger have been a subject of great attention among applied mathematicians, heat transfer, and fluid dynamics analysts due to the numerous engineering applications.

Improving the thermal performance of heat exchangers can be achieved by adopting several techniques. These techniques can be categorized into three groups: active, passive, and compound techniques [1-6]. In the active techniques, thermal performance of heat exchanger is improved by introducing additional external energy to the fluid such as vibrating the surface, induced pulsation, well stirring the fluid, mechanical aids, etc. In the passive techniques, this improvement is acquired without giving any additional energy and uses geometrical modifications to the flow channel such as rough surfaces, extended surfaces, coiled tubes, swirl flow devices, additives for fluids (e.g., nanofluids), and many others. In the compound techniques, the active and passive techniques may be employed simultaneously. The use of swirl flow devices and nanofluids methods are the most common types of passive techniques used in the thermal enhancement of heat exchangers. Swirl flow devices are designed to create a rotational motion around the axis of the axial flow direction, so the residence time and path length of flow are increased, thereby augmenting the heat transfer process. The swirl flow can be created in tubes by two types: the continuous and decaying swirl flow devices. In the continuous swirl flow devices, the swirling exists over the entire length of the tube such

as twist tape and wire coil inserts [7-18], while in the decaying swirl flow devices, the swirl is produced at the entrance of the tube and decays along the flow path such as tangential flow injection slots, the guide blade, and the snail swirl generators [19-29]. Several studies have investigated heat transfer improvement and flow field inside the tube using the continuous swirl flow such as twisted tape and wire coil inserts [7-18]. They noticed that the inserts improve the heat transfer at a cost of rising in pressure drop. The thermo-hydraulic performance of wire coil is good compared with twisted tape in turbulent flow and vice versa in the case of laminar flow. A more comprehensive review of the twisted tape and wire coil inserts can be viewed with details in Refs. [2-6].

The turbulent decaying swirl flow in a tube has been studied to understand the physics and behaviour of the swirling flow in Refs. [19-26]. They found that the heat transfer is augmented, the turbulent viscosity is typically non-isotropic and the RSM turbulence model is the most appropriate approach to model Reynold's stress [24-26]. There were few studies on the decaying swirl flow through a heat exchanger especially in the case of the use of tangential flow injection slots as a swirl generator. Durmus et al. [27] investigated experimentally the heat transfer and pressure drop in a concentric double pipe heat exchanger with snail entrance for parallel and counter flow. The results revealed that the heat transfer is enhanced up to 120% with a slight increase in pressure drop. Eiamsa-ard et al. [28] studied experimentally the heat transfer and friction factor in a heat exchanger tube equipped with propeller type swirl generators. The results showed that the heat transfer coefficient is about 1.2 times over the plain tube and the friction factor is found to be 3-18 times over the plain tube. The effects of propeller-type turbulators located in the inner pipe of heat exchanger on entropy generation rate and exergy loss rate were investigated experimentally by Kurtbas et al. [29]. It was seen that Nusselt number and exergy loss rate approximately increase from 95 to 354 and 0.04 to 0.2, respectively. Efficiency of the heat exchanger changed between 0.17 to 0.72 levels.

Heat exchanger performance can be improved by increasing the heat transfer properties of the fluid. To increase the properties of a fluid, small solid particles of a material with high thermal conductivity in the nanoscale range are added to that fluid which is known as nanofluid. Nanofluids are new class of heat transfer fluids and are produced by suspending nanometre-sized particles (< 100 nm) in conventional heat transfer fluids. Nanofluids were used in various engineering and industrial applications for their high thermal performance [30-32]. In 1995, Choi and Eastman [33] first proposed the concept of nanofluids. In the past few years, the use of nanofluids to enhance heat transfer has attracted great attention from researchers and scientists. The first empirical correlation for predicting the nanofluid Nusselt number was proposed by Pak and Cho [34] who investigated the turbulent heat transfer and friction factor of TiO_2-water and Al_2O_3-water nanofluids with various concentrations in a circular tube. It was assumed that the nanofluid mixture can be considered a single- phase liquid and the properties such as thermal conductivity and viscosity were calculated on this basis. The results showed that Nusselt number of nanofluids increases with increasing volume concentration and there was an additional pumping penalty. Also Sunder et al. [35] examined the turbulent heat transfer behavior of Al_2O_3/water nanofluids with various concentrations in a circular tube with and without twist tape insert at constant heat flux boundary. The properties of nanofluid were calculated with the equation given by Pak and Cho [34]. The results revealed that a maximum enhancement of 28% has been observed compared to pure water. Murali et al. [36] studied the heat transfer and pressure drop of turbulent flow in a circular tube fitted with trapezoidal cut twisted tape insert using Fe_3O_4 nanofluid. The heat transfer rate was 78.6% higher than the plain tube, the friction factor was 3.352 times greater than the plain tube and the performance ratio was more than unity. Hussein et al. [37] investigated the effect of TiO_2-water nanofluid on heat transfer enhancement under turbulent flow in an elliptical tube. The FLUENT code was used to solve the governing equations of flow and it was assumed that the nanofluid mixture can be considered a single-phase liquid. The effect of volume concentration and diameter of nanoparticles on heat transfer and friction factor was reported. The results showed that the Nusselt number and friction factor increase with increasing volume concentrations and decreasing diameters of nanoparticles. Jassim and Ahmed [38] experimentally investigated the influence of two different nanofluids (Cu/water and Al_2O_3/water) on the performance of a double pipe heat exchanger at different volume concentrations and Reynolds number. The results showed a significant improvement in the Nusselt number up to 13% for Al_2O_3 and 23% for Cu. Bahmani et al. [39] numerically investigated the heat transfer of Al_2O_3/water nanofluid in a double pipe heat exchanger. The governing equations have been solved using a FORTRAN code, single-phase and standard k-ε models have been used for nanofluid and turbulent modelling. The results indicated that by increasing the

nanoparticles volume concentration the Nusselt number and convection heat transfer coefficient is enhanced. Maximum average Nusselt number and thermal efficiency enhancement were 32.7% and 30%, respectively. Duangthongsuk and Wongwises [40, 41] studied experimentally the heat transfer enhancement and pressure drop characteristics of TiO_2-water nanofluid in a double pipe counter flow heat exchanger under turbulent flow conditions. The results showed that at a volume concentration less than 2.0%, the maximum heat transfer coefficient of nanofluids was approximately 26% greater than that of pure water, while at a volume concentration of 2.0% the heat transfer coefficient was approximately 14% lower than that of base fluids. The pressure drop of nanofluids was slightly higher than the base fluid and increases with increasing the volume concentrations. Gkountas et al. [42] presented an investigation on the thermal behaviour of a heat exchanger, used as a precooler by employing an Al_2O_3-water nanofluid as a coolant. An analytical one-dimensional model was developed to examine the heat transfer. It was shown that as the nanoparticle concentration increases, the effectiveness of the heat exchanger was enhanced up to 2.5% for a range of nanoparticle volume fractions 0-5%. The heat transfer coefficient was improved by about 75% at a volume concentration of 5% with the heat exchanger length reduced up to 1%, while the pressure drop increased up to 8% as compared with the pure water case.

The main aim of this study is to numerically investigate the influences of nanofluids on the thermal and hydrodynamic behaviours of double pipe counter flow heat exchanger equipped with a decaying swirl flow system using ANSYS FLUENT 15 [43]. The swirl flow is generated using a tangential slot at the flow inlet of the outer pipe with a tangent angle of 30º. Nanofluids used in this study are formed by adding nanoparticles of Al_2O_3, CuO, TiO_2, and ZnO with water. The effects of volume concentrations, nanomaterial types, and diameters of nanoparticles are considered.

2. Numerical Method

2.1. Geometry Modelling

The proposed schematic diagram of the double pipe heat exchanger under study is shown in Fig. 1. In this design, a single slot placed tangentially at the flow inlet of the outer pipe of heat exchanger with a tangent angle of 30°. This slot is used to generate a decaying swirl flow through the annular of the heat exchanger. The tangent angle of slot is measured between slot axis and the axial direction. The cold fluid whether pure water or nanofluid is flowing through the annulus whose mass flow rate is varied whereas hot water is flowing through the inner pipe axially whose mass flow rate is constant, and this value corresponds to Re=13059. The inlet temperatures of cold and hot fluid are constant at 29.04 and 54.66 ºC, respectively. The inner pipe material type is copper and has a 19 mm diameter (di) with neglecting the thickness, while the outer pipe has a 56 mm diameter ($D_{i)}$ with neglecting the thickness and it's thermally insulated assuming there is no heat loss in the system, and the total length of the heat exchanger is 2000 mm.

2.2. Thermophysical Properties of Nanofluids

The nanofluid behaves more like a single-phase fluid as a result of the suspended particles are infinitesimal (less than 100 nm) so the nanofluid can be modelled as a single-phase approach. Nanoparticles used in this study are Aluminium Oxide (Al_2O_3), Copper Oxide (CuO), Zinc Oxide (ZnO), Titanium Dioxide (TiO_2). Nanofluids are formed by adding nanoparticles (p) with a base fluid (f) which is water. The thermophysical properties of nanofluids such as density (ρ_{nf}), specific heat (Cp_{nf}), thermal conductivity (λ_{nf}), and dynamic viscosity (μ_{nf}) are determined by employing well-known empirical correlations [37,44].

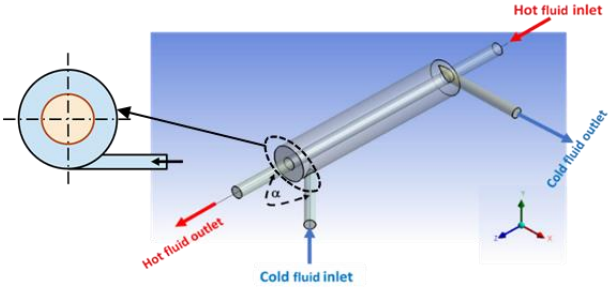

Fig. 1. The 3-D proposed designs of the heat exchanger (Tangential slot with a tangent angle of 30°).

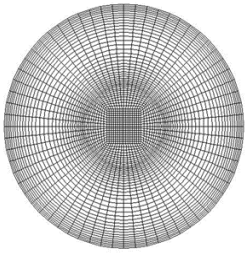

Fig. 2. Surface mesh of heat exchanger.

$$\rho_{nf} = \phi\rho_p + (1-\phi)\rho_f \quad (1)$$

$$c_{p_{nf}} = \frac{\phi(\rho c_p)_p + (1-\phi)(\rho c_p)_f}{\rho_{nf}} \quad (2)$$

$$\frac{\lambda_{nf}}{\lambda_f} = 0.8938(1+\phi)^{1.37}\left(1+\frac{T_{nf}}{70}\right)^{0.2777}\left(1+\frac{d_p}{150}\right)^{-0.0336}\left(\frac{\alpha_p}{\alpha_f}\right)^{0.01737} \quad (3)$$

$$\frac{\mu_{nf}}{\mu_f} = (1+\phi)^{11.3}\left(1+\frac{T_{nf}}{70}\right)^{-0.038}\left(1+\frac{d_p}{170}\right)^{-0.061} \quad (4)$$

Where; ϕ: volume concentration $= \frac{V_p}{V_p+V_f}$, d_p: particle size (nm), T_{nf} : nanofluid temperature (°C) and α: thermal diffusivity (m^2/s), subscripts *f*, *p*, and *nf* are represented base fluid, nanoparticles and nanofluid properties.

Equations (3) and (4) are valid for nanoparticles having a volume concentration less than 4.0%, temperature of 20-70 °C and size in the range of 20-150 nm. The values of thermophysical properties of water and nano materials are shown in Table 1.

Table (1) The values of thermophysical properties of water and nano materials.

The thermophysical properties of water and different nano materials at T=30 °C.					
Thermo-physical properties	Water	Al_2O_3	CuO	ZnO	TiO_2
Density, ρ (kg/m^3)	995.025	3600	6500	5600	4250
Dynamic viscosity, μ (Pa.s)	0.00077	-	-	-	-
Thermal conductivity, λ (W/m.K)	0.62	36	20	13	8.953
Specific heat, C_p (J/kg.K)	4178	765	535.6	495.2	686.2

2.3. Governing Equations

The thermal and hydrodynamic characteristics of heat exchanger are simulated based on Reynolds Averaged Navier-Stokes (RANS) and energy equations. The flow in heat exchanger is assumed to be turbulent incompressible, and steady three-dimensional. The radiation, gravity and viscous heating effect are neglected. The single-phase approach is adopted for nanofluid modelling. The thermophysical properties of cold and hot fluids are constant corresponding to their inlet temperatures. Based on the above assumptions, the continuity, momentum, and energy equations can be expressed in the tensor form as follows:

Continuity Equation:

$$\frac{\partial u_i}{\partial x_i} = 0 \quad (5)$$

Momentum Equation:

$$\frac{\partial(u_i u_j)}{\partial x_j} = -\frac{\partial p}{\partial x_i} + \frac{\partial}{\partial x_j}\left(\mu\frac{\partial u_i}{\partial x_j}\right) + \frac{\partial}{\partial x_j}\left(-\rho\overline{\acute{u}_i\acute{u}_j}\right) \quad (6)$$

Energy Equation:

$$\rho c_p \frac{\partial}{\partial x_i}(u_i T) = \frac{\partial}{\partial x_i}\left[\left(\lambda + \frac{\mu_t c_p}{Pr_t}\right)\left(\frac{\partial T}{\partial x_i}\right)\right] \quad (7)$$

Where; ρ, c_p, λ, μ are density, specific heat, thermal conductivity and dynamic viscosity of the fluid, respectively. The turbulent Prandtl number Pr_t is computed based on the turbulent viscosity μ_t. The term, $-\rho\overline{\acute{u}_i\acute{u}_j}$ in Eq. (6) is called the Reynolds stress tensor and u_i, $\acute{u}_i$ represent the mean and fluctuating velocity component in *i*-direction. These equations are not a closed set and turbulence models are required to model the Reynolds stress tensor. In the study of swirl flow, the RSM turbulence model was the most appropriate approach to model Reynolds's stress [24-26]. Thus, the RSM with quadratic pressure-strain turbulence model is used in this CFD simulation. The RSM models solve the Reynolds stresses transport equations individually. The term of the pressure strain in this model can be modelled accordingly to Quadratic Pressure-Strain Model. Detailed description of the RSM turbulence model can be found in ANSYS FLUENT 15 [43].

2.4. Boundary Conditions

Cold liquid (pure water or nanofluid) passes through the annular side while hot water passes through the inner pipe. Therefore, there are boundary conditions for both cold and hot flow used in this geometry domain which are:

At inlets: for hot flow, the mass flow rate is constant, and this value corresponds to Re=13059 and temperature is set constant; while for cold flow, the mass flow rate is varied, and temperature is set constant.

At the outlet: Atmospheric pressure outlet condition is applied for both cold and hot flow.

At the inner wall: the surface interface between cold and hot flows was set to couple wall for thermal condition.

At the outer wall: the outer wall was set to adiabatic condition.
For all walls, no-slip boundary conditions are specified with wall function approach. The non-equilibrium wall functions are recommended for use in complex flows involving separation, reattachment, and impingement where the mean flow and turbulence are subjected to pressure gradients and rapid changes [43, 45].

2.5. Numerical Procedures

The CFD simulation was conducted by solving the set of governing equations accompanied with the boundary conditions using the FLUENT software code. The governing equations are discretized using the control volume-based approach. The SIMPLE algorithm is employed for pressure velocity coupling and the second-order upwind differencing scheme is applied for pressure, momentum, turbulent dissipation rate, and energy while in Reynolds stresses equations the first-order upwind is used. The simulation has been carried to reach 10^{-4} residual errors of continuity, momentum, and turbulence.

3. Data Reduction Equations

The heat transfer rate can be calculated as:

For hot fluid path: $$Q_h = \dot{m}_h C_{p_h}(T_{hi} - T_{ho}) \quad (8)$$

For cold fluid path: $$Q_c = \dot{m}_c C_{p_c}(T_{co} - T_{ci}) \quad (9)$$

The Reynolds number can be calculated from the following equation:

For hot fluid flow (inner pipe), $$Re = \frac{4\dot{m}_h}{\pi d_i \mu_h} \quad (10)$$

For cold fluid flow (annular), $$Re = \frac{4\dot{m}_c}{\pi(D_i - d_i)\mu_c} \quad (11)$$

where, $\dot{m}_h, \dot{m}_c$ and μ_h, μ_c are the mass flow rates and dynamic viscosity of the hot and cold water. d_i, and D_i are the inner diameter of the inner pipe, and the inner diameter of the outer pipe.

The effectiveness of the heat exchanger can be calculated by: $$\epsilon = Q/Q_{max} \quad (12)$$

Where Q_{max} is the maximum heat transfer rate that can be obtained from the heat exchanger and defined as,

$$Q_{max} = \left(\dot{m}C_p\right)_{min}(T_{hi} - T_{ci}) \quad (13)$$

The average heat transfer coefficient (h) of cold fluid is computed from the following equation:

$$h = \frac{q}{T_{wall} - T_c} \quad (14)$$

Where q is the average heat flux, T_{wall} is the average wall temperature, and T_c is the bulk temperature of the cold water.

4. Grid Studying and Numerical Model Validation

Before performing CFD simulation, a grid independence study should be first analyzed to determine the effects of grid sizes on the results. ANSYS design modeler is used to create the 3-D heat exchanger geometry and structured mesh was formed by using ANSYS meshing as seen in Fig. 2. Three different meshes were examined, namely 1.6, 2.5, and 3.4 million cells, respectively. Figure 3 shows the local distribution of cold temperature along the heat exchanger at Re= 13059 and 22076 for hot and cold-water flow, respectively. It was seen that the 2.5 and 3.4 million cells perform nearly identical results. To reduce the computational time, a mesh with 2.5 million cells was applied for the simulation.

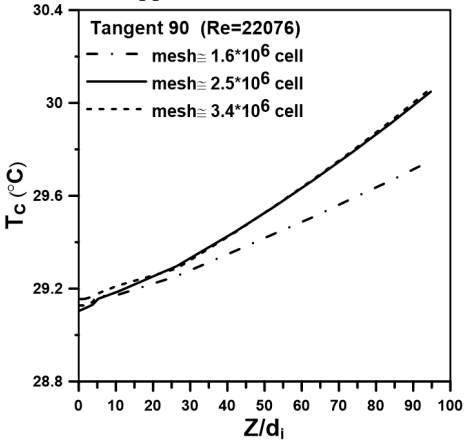

Fig. 3. Effect of grid size on the distribution of cold water temperature.

The validation of the numerical model was performed based on the geometry and boundary conditions which was employed in the experimental work of Duangthongsuk and Wongwises [41] and also comparison by the correlation which was developed by Gnielinski and Petukhov [46]. For the previous experimental data, the cold water passes through the inner pipe with an inlet temperature of 25 ºC and various flow rates, while the hot water passes through the annulus side with an inlet temperature of 35 ºC and flow rate of 3 LPM. The average heat transfer coefficient (h) and pressure drop (ΔP) of the inner tube were computed and compared with the previous works. As illustrated in Fig. 4, the predicted results for heat transfer coefficient and pressure drop of double pipe heat exchanger show acceptable agreement with

the available reported empirical correlation and experimental data.

5. Results and Discussion

In the following sections, the effect of volume concentration, nanomaterial types, and nanoparticles size on the performance of the double pipe heat exchanger under study is presented. Nanofluids used in this study are formed by adding nanoparticles with water. Four different types of nanoparticles, Al2O3, CuO, TiO2 and ZnO, the volume concentration in the range of 0% to 3% and different nanoparticle diameters in the range of 20 nm to 50 nm are used.

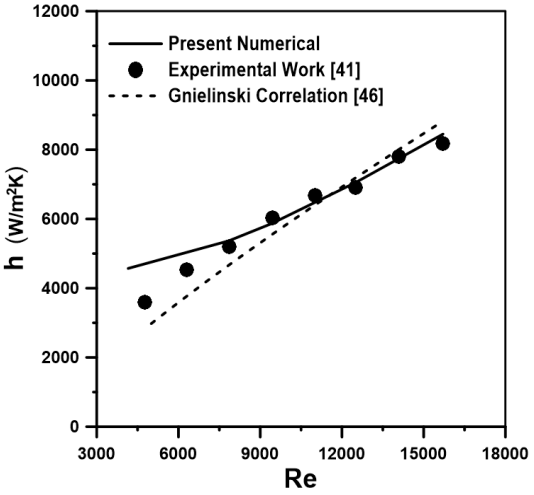

(a) average heat transfer coefficient (h)

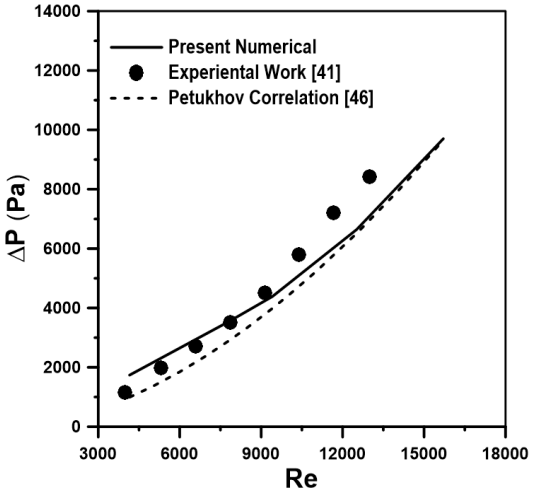

(b) Pressure drop (ΔP)

Fig. 4. Comparison between present results and previous results.

5.1. Effect of Nanoparticles Volume Concentrations

The influence of nanoparticles volume concentrations (ϕ) of Al_2O_3+water nanofluid at 32 nm particles diameter is discussed in this section. The different nanoparticles volume concentration (ϕ) tested in this study range from 0% to 3%. Figures 5 shows the variation of average heat transfer coefficient with Reynolds number at different nanoparticles volume concentration (ϕ) of swirl flow case and its comparison with the axial flow case using pure water. From the figure, it can be observed that the heat transfer increases with increasing Reynolds number for all cases. The swirl flow causes a secondary flow that increases turbulence level and disturbs the thermal boundary layer. Therefore, the heat transfer of the swirl flow case is improved compared to the axial flow case. The influence of using nanofluids on the heat transfer is significant for all the Reynolds number. At the comparable Reynolds number, the heat transfer using nanofluids with different volume concentrations is considerably higher than that of pure water (ϕ=0) and axial flow case which indicated the enhanced heat transfer. The thermal conductivity of the nanofluid is improved due to the addition of solid nanoparticles to the base fluid, and thus the heat transfer is enhanced. The heat transfer is also enhanced due to the interaction of the nanoparticles with the base fluid that creates breakdown of the boundary layer as a result of the development of the turbulence intensity [38]. The value of average heat transfer coefficient for the Al_2O_3 nanoparticles with a volume concentration of ϕ=3% is 14% higher in comparison to those of pure water (ϕ=0%).

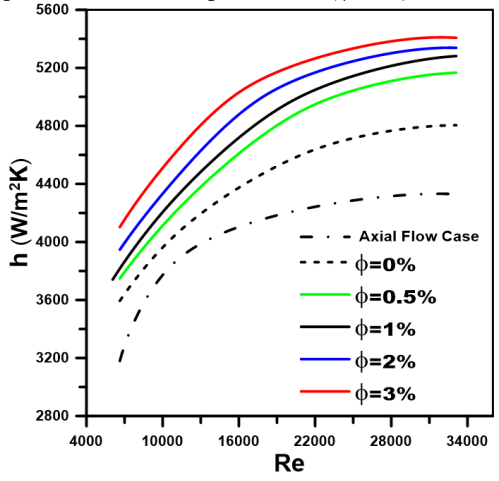

Fig. 5. Average heat transfer coefficient variation with Reynolds number at a different volume concentration of Al_2O_3.

The effect of volume concentrations on the axial distribution of the local heat transfer coefficient at Re=6622 is shown in Fig. 6. Comparison has been done for ϕ= 0, 2 and 3%. It can clearly be seen that the local heat transfer coefficient resulting from the use of nanofluid at different volume concentrations is significantly higher than those of pure water (ϕ=0) along the heat exchanger. The local heat transfer coefficient increases with the increase of volume concentration. The local heat transfer coefficient is enhanced as a result of improving the properties of nanofluids as well as increasing the effective surface of particles with increasing volume concentration. The peaks that appear in the heat transfer coefficient are due to the existence of swirling flow.

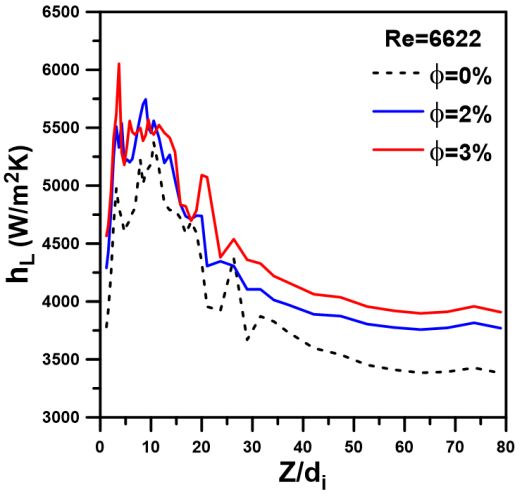

Fig. 6. Effect of particles volume concentration of Al_2O_3 on the local heat transfer coefficient for slot with tangent angle of 30° case at Re=6622.

Figure 7 shows the axial distribution of hot water and inner pipe wall temperature along the heat exchanger at Re=6622 and volume concentration of Al_2O_3 at 0, 2 and 3%. In this case of counter flow heat exchanger, the hot water enters from the right side and the cold nanofluid enters from the left side. It can be seen from this figure the temperature of hot water as well as inner pipe wall temperature decrease along the heat exchanger as a result of the heat exchange between the cold fluid and hot water for all volume concentration. By increasing the volume concentration of Al_2O_3 nanoparticles, the hot water as well as inner pipe wall temperature is cooled more than pure water. Two factors that have a direct effect on temperature are the thermal conductivity and heat capacity of the nanofluid. The thermal conductivity is improved, and the heat capacity reduces with increasing the volume concentration. Therefore, the heat exchange between the two fluids is high, and the cold nanofluid absorbs more heat from the hot water.

The evolution of heat exchanger effectiveness with Reynolds number for different nanoparticles volume concentration of swirl flow as well as the case of axial flow is shown in Figs. 8. Due to the high thermal conductivity of the nanofluid, the effectiveness of the heat exchanger increases with increasing volume concentration. The effectiveness of heat exchanger is dependent on the heat transfer, therefore, increasing the heat transfer affects the effectiveness of the heat exchanger as depicted in this figure.

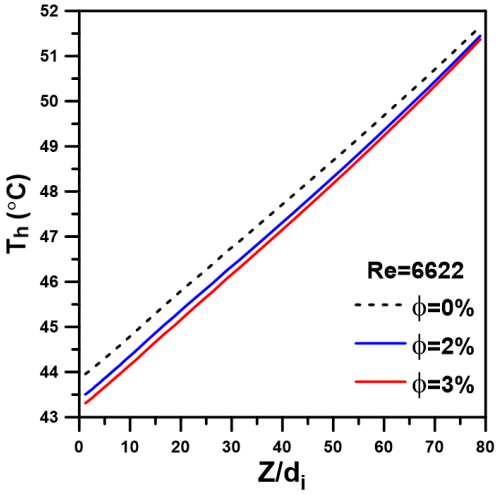

(a) Temperature of hot water

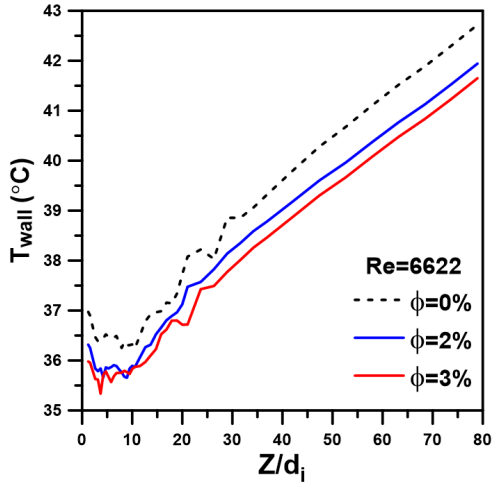

(b) Temperature of inner pipe wall

Fig. 7. Effect of particles volume concentrations of Al_2O_3 on the axial distribution at Re=6622.

The variation of the pressure drop with Reynolds number at a different nanoparticles volume concentration (ϕ) of swirl flow case and its comparison with the axial flow case using pure water is presented in Fig. 9. It is observed that the pressure drop increases with increasing Reynolds number and nanoparticles volume concentration. Pressure drop with the presence of swirl flow is higher than that in the case of axial flow due to flow resistance (high wall friction). The pressure drop for the different volume concentration of nanofluid is higher than that for pure water. The pressure drop increases as a result of the addition of nanoparticles to the base fluid. The addition of nanoparticles increases fluid viscosity and flow resistance thus increasing friction which diminishes the fluid motion. The nanofluid flows through the annulus of the heat exchanger and the nanoparticles impinge with the wall of inner and outer pipe resulting in an increase in the contact area of the flow, thus increasing the wall friction which leads to an increase in pressure drop. The values of pressure drop for the Al_2O_3 nanoparticles are 5% and 72% of pure water at ϕ=0.5% and ϕ=3%, respectively.

5.2. Effect of Nanomaterial Types

In this section, the effect of different types of nanoparticles namely Al_2O_3, CuO, TiO_2, and ZnO for volume concentration of ϕ=1% and diameter of d_p=32 nm is discussed. The variation of the average heat transfer coefficient and effectiveness of the heat exchanger with Reynolds number at different types of nanofluids and pure water is illustrated in Fig. 10 (a) and (b). It can be clearly seen that the average heat transfer coefficient and effectiveness increases significantly with increasing Reynolds number for all types of nanofluids under study. The Al_2O_3 nanofluid has the highest average heat transfer coefficient and effectiveness, followed by CuO, ZnO, and TiO_2 respectively. This is because the Al_2O_3 nanofluid has the highest thermal conductivity and lowest density compared with all the other nanofluids. The fluids with the lowest density have the highest velocity, which increases heat convection. The highest thermal conductivity and velocity represent the main reasons for enhancing the heat transfer coefficient and effectiveness of the heat exchanger.

It is indicated that increasing the velocity has a significant influence on improving the heat transfer. In order to illustrate the influence of nanofluid velocity on the heat transfer, the CFD simulation predicted the velocity magnitude in the annulus of heat exchanger for different nanoparticle types at Re=33114 and a cross section of Z=500 mm, as shown in Fig. 11. It can be clearly seen that from the contour of velocity, the Al_2O_3 nanofluid has the highest velocity due to its lower density followed by CuO, ZnO, and TiO_2 and pure water. The higher velocity increases thermal convection, therefore improving the heat transfer.

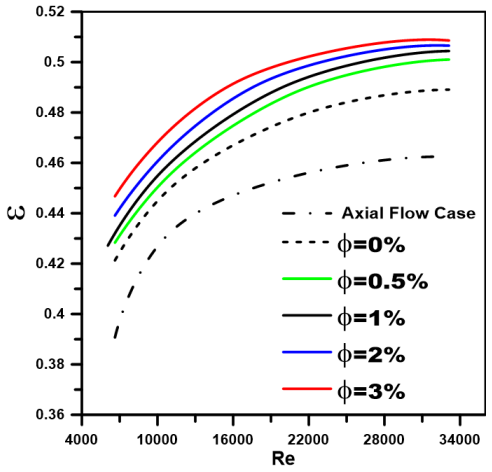

Fig. 8. Effectiveness of heat exchanger variation with Reynolds number at a different volume concentration of Al_2O_3.

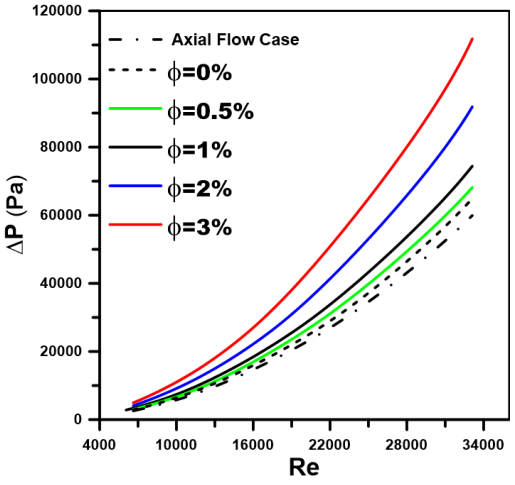

Fig. 9. Pressure drop variation with Reynolds at a different volume concentration of Al_2O_3.

Figure 12 shows the effect of different nanoparticle types on the hot water and inner wall temperature for Re=33114 at Z=500 mm. The results indicate that the temperature of hot water and inner wall of Al_2O_3 nanoparticles is low compared to other nanoparticles and pure water. The lower hot water and inner wall temperature corresponds to the higher heat transfer. This means that the thermal exchange

between the cold and hot fluid is high i.e., the heat transfer is enhanced for all nanofluids compared to pure water.

The variation of pressure drop with Reynolds number at different types of nanofluids and pure water is demonstrated in Fig. 13. It is observed that the pressure drop increases with increasing Reynolds number. The addition of nanoparticles to the base fluid causes a slight increase in the pressure drop compared to pure water. The nanoparticles increase the fluid viscosity thus increasing wall friction which leads to an increase in pressure drop. In comparison between different types of nanofluids, there is no significant change in pressure drop because the viscosity of the nanofluids is close to each other.

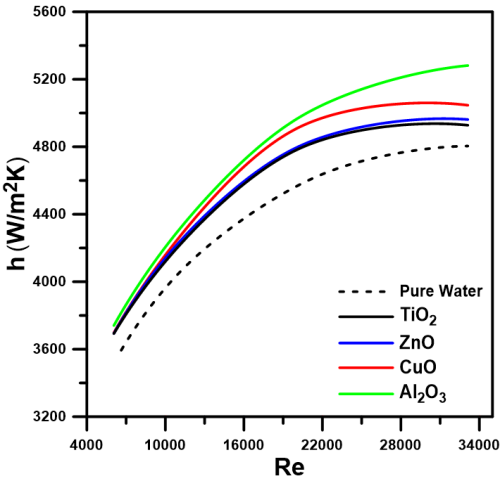

(a) average heat transfer coefficient

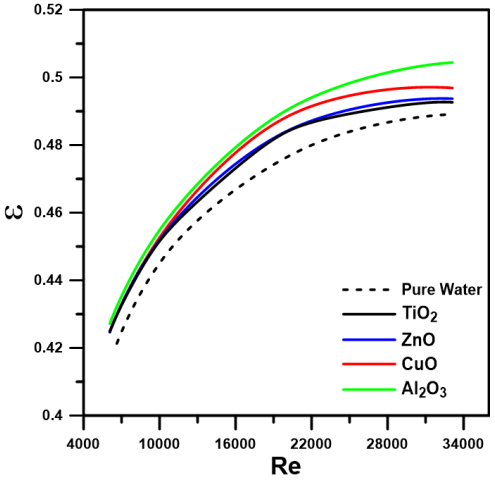

(b) Effectiveness

Fig. 10. The effect of nano material types with Reynolds number.

5.3. Effect of Nanoparticle Diameters

The effect of different nanoparticle diameters (d_p) of Al_2O_3+water nanofluid at volume concentration of ϕ=3% on the thermal performance of heat exchanger is discussed in this section. The different nanoparticle diameters (d_p) tested in this study are 20, 32, and 50 nm.

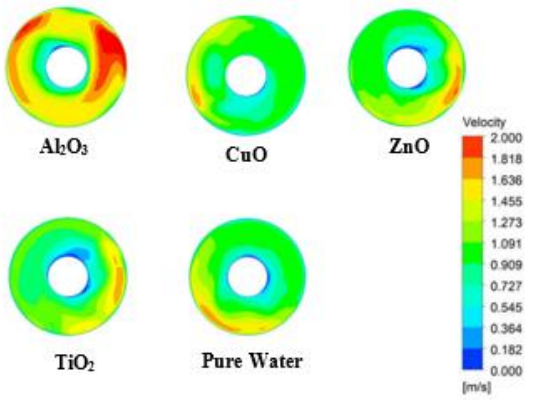

Fig. 11. The contours of velocity in the heat exchanger annulus of different nanoparticle types for Re=33114, ϕ=1%, d_p=32 nm at Z=500 mm.

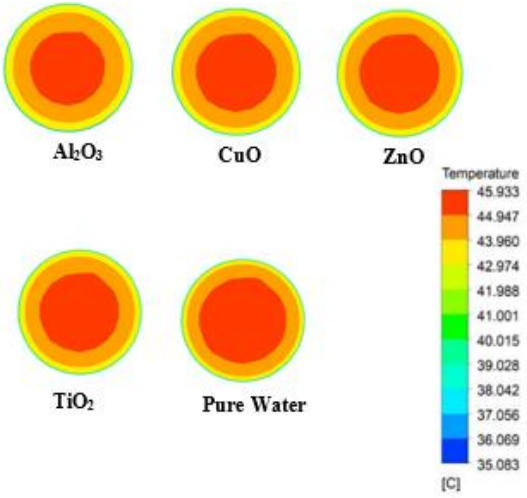

Fig. 12. The contours of temperature in the inner pipe of heat exchanger of different nanoparticle types for Re=33114, ϕ=1%, d_p=32 nm at Z=500 mm.

Figure 14 (a) and (b) shows the effect of different nanoparticle diameters on the average heat transfer coefficient and effectiveness of heat exchanger with different Reynolds numbers at 3% volume concentration of the Al2O3+water nanofluid. The results revealed that the average heat transfer coefficient as well as effectiveness increases

significantly with increasing Reynolds number for all nanoparticle diameters under study. The average heat transfer coefficient as well as effectiveness increases as the particle diameter decreases. As the particle diameter decreases, the surface area per unit volume increases, the heat transfer depends on the surface area, so the efficiency of heat transfer from the nanoparticles to the base fluid increases. In addition, the Brownian motion velocity of smaller particles is higher, which again increases the contribution of the nanoparticles to the total heat transfer by continuously creating additional paths for heat flow in the fluid.

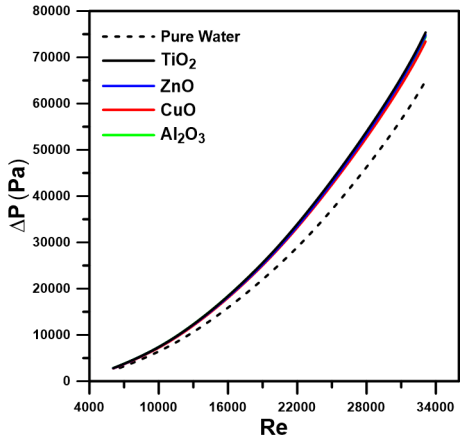

Fig. 13. The effect of nano material types with Reynolds number on the pressure drop.

The effect of different nanoparticle diameters on the average outlet temperature of hot water as well as the average temperature of inner pipe wall of heat exchanger with different Reynolds numbers is depicted in Fig15 (a) and (b). It is clearly seen that the outlet temperature of the hot water, as well as the temperature of the inner pipe wall of the heat exchanger decrease with increasing the Reynolds number for all values of nanoparticle diameters. As mentioned previously, as the particle diameter decreases, the surface area increases thus the thermal exchange between the cold and hot fluid increases resulting in cooling of both the hot fluid and the inner wall. The nanoparticle diameter of 20 nm has the lowest temperature, while the nanoparticle diameter of 50 nm has the highest temperature, as shown in this figure.

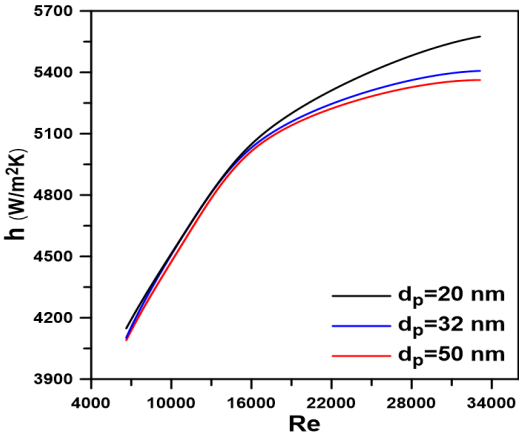

(a) average heat transfer coefficient

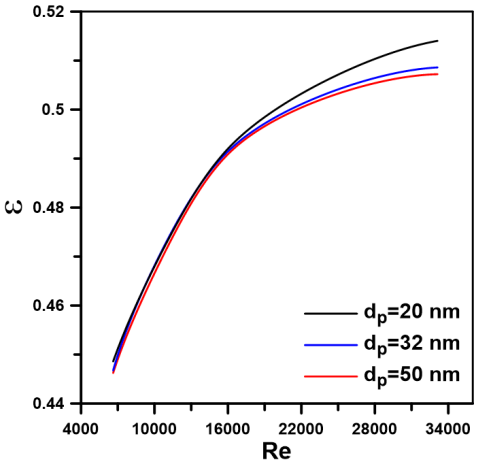

(b) Effectiveness

Fig. 14. The effect of nanoparticle diameters with Reynolds number

The influence of different nanoparticle diameters of Al_2O_3+water nanofluid on the pressure drop with Reynolds numbers is illustrated in Fig. 16. The results indicate that the pressure drop increases with increasing the Reynolds number and there is a slight variation in the pressure drop when nanoparticle diameters of Al_2O_3+water nanofluid are changed, as presented in the figure.

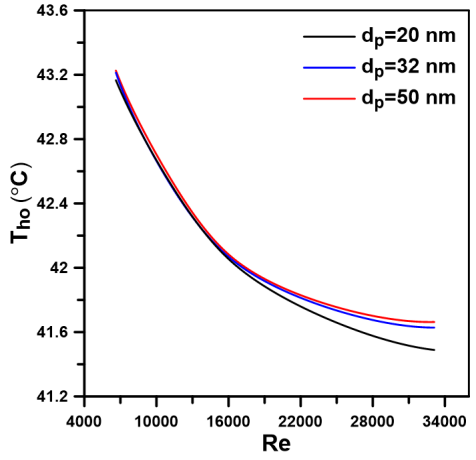

(a) Outlet temperature of hot water

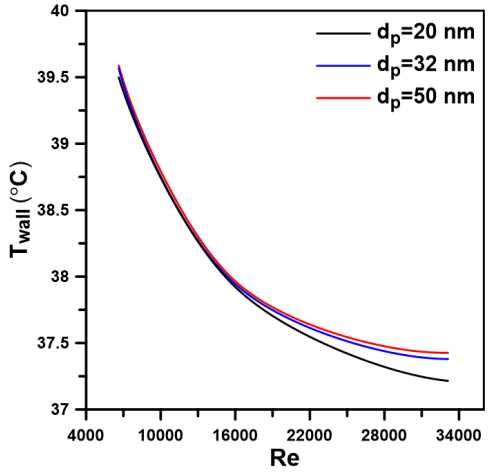

(b) Temperature of inner pipe wall.

Fig. 15. Average temperature variation with Reynolds number at a different nanoparticle diameter of Al_2O_3.

6. Conclusions

The influence of nanofluids on the thermal and hydrodynamic behaviours of double pipe counter flow heat exchanger equipped with a decaying swirl flow system is numerically investigated. The swirl flow is generated using a tangential slot at the flow inlet of the outer pipe with a tangent angle of 30º. Nanofluids used in this study are formed by adding nanoparticles with water. Four different types of nanoparticles, Al_2O_3, CuO, TiO_2 and ZnO, the volume concentration in the range of 0% to 3% and different nanoparticle diameters in the range of 20 nm to 50 nm are used. The following main conclusions can be drawn from the obtained study.

1. The heat transfer rate and pressure drop increase with increasing Reynolds number and volume concentrations of nanofluids under study.
2. All nanofluid types achieve better heat transfer enhancement compared to pure water, but with slight increases in pressure drop. The Al_2O_3 nanomaterial has better thermal enhancement characteristics followed by CuO, ZnO, and TiO_2, respectively.
3. By increasing the volume concentration of nanofluid, the heat transfer as well as pressure drop increase.
4. The heat transfer as well as effectiveness increase with decreasing the particle diameter and there is a slight variation in the pressure drop.
5. The nanoparticles improve thermal conductivity of base fluid and that the nanoparticle size, as well as the concentrations of the nanoparticles plays a major role in the effectiveness of the nanofluids.

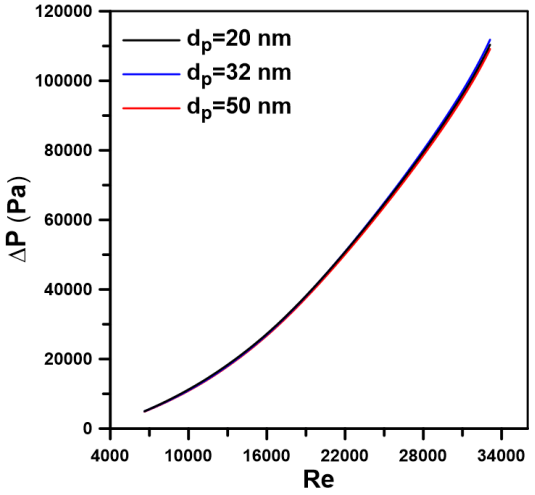

Fig. 16. The effect of nanoparticle diameters with Reynolds number on the pressure drop.

References

[1] A. E. Bergles, Heat transfer enhancement-the encouragement and accommodation of high heat fluxes, J Heat Transfer (Trans ASME), 119, 8-19 (1997).

[2] S. Liu and M. Sakr, A comprehensive review on passive heat transfer enhancements in pipe exchangers, Renewable and Sustainable Energy Reviews, 19, 64-81(2013).

[3] T. Alam and M. Kim, A comprehensive review on single phase heat transfer enhancement techniques in heat exchanger applications,

Renewable and Sustainable Energy Reviews, 81, 813-839 (2018).

[4] N. C. Kanojiya, V.M. Kriplani and P. V. Walke, Heat transfer enhancement in heat exchangers with inserts: A review, Int. J. Eng. Research Technology (IJERT), 3, 494-500 (2014).

[5] A. Dewan, P. Mahanta, K. Sumithra Raju and P. Suresh Kumar, Review of passive heat transfer augmentation techniques, Proc. Instn Mech. Engrs Part A: J. Power and Energy, 218, 509-527 (2004).

[6] A. H. Yousif and M. R. Khudhair, Enhancement heat transfer in a tube fitted with passive technique as twisted tape insert – A comprehensive review, American Journal of Mechanical Engineering, 7, 20-34 (2019).

[7] S. K. Saha and A. Dutta, Thermo-hydraulic study of laminar swirl flow through a circular tube fitted with twisted tapes, Trans. ASME, J. Heat Transfer, 123, 417-421 (2001).

[8] S. K. Saha and K. Bhunia, Heat transfer and pressure drop characteristics of varying pitch twisted-tape-generated laminar smooth swirl flow, In Proceedings of 4th ISHMT-ASME Heat and Mass Transfer Conference, India (Tata McGraw-Hill, New Delhi), 423-428 (2000).

[9] S. K. Saha, A. Dutta and S. K. Dhal, Friction and heat transfer characteristics of laminar swirl flow through a circular tube fitted with regularly spaced twisted-tape elements, Int. J. Heat and Mass Transfer, 44, 4211-4223 (2001).

[10] M. M. K. Bhuiya, A. S. M. Sayem, M. Islam, M. S. U. Chowdhury and M. Shahabuddin, Performance assessment in a heat exchanger tube fitted with double counter twisted tape inserts, Int. Comm. Heat Mass Transfer, 50, 25–33 (2014).

[11] N. Piriyarungrod, Manoj Kumar, C. Thianpong, M. Pimsarn, V. Chuwattanakul, S. Eiamsa-ard, Intensification of thermo-hydraulic performance in heat exchanger tube inserted with multiple twisted-tapes, Applied Thermal Engineering, 136, 516-530 (2018).

[12] P. Bharadwaj, A. D. Khondge, and A. W. Date, Heat transfer and pressure drop in a spirally grooved tube with twisted tape insert, Int. J. Heat and Mass Transfer, 52, 1938-1944 (2009).

[13] S. Gunes, V. Ozceyhan, and O. Buyukalaca, Heat transfer enhancement in a tube with equilateral triangle cross sectioned coiled wire inserts, Experimental Thermal and Fluid Science, 34, 684-691 (2010).

[14] M. Saeedinia, M. A. Akhavan-Behabadi and M. Nasr, Experimental study on heat transfer and pressure drop of nanofluid flow in a horizontal coiled wire inserted tube under constant heat flux, Experimental Thermal and Fluid Science, 36, 158-168 (2012).

[15] A. E. Zohir and M.A. Habib, Heat transfer characteristics in a double-pipe heat exchanger equipped with coiled circular wires, Journal of Engineering Sciences, Assiut University, 40,731-744 (2012).

[16] I. A. H. Salih, Thermal characterization of turbulent flow in a tube with discrete coiled wire insert, Journal of Engineering and Development, 18, 126-143 (2014).

[17] L. Wang and B. Sunden, Performance comparison of some tube inserts, Int. Comm. Heat Mass Transfer, 29, 45-56 (2002).

[18] S. S. Choudhari and S. G. Taji, Experimental studies on effect of coil wire insert on heat transfer enhancement and friction factor of double pipe heat exchanger, International Journal of Computational Engineering Research, 3, 32-39 (2013).

[19] O. Kitoh, Experimental study of turbulent swirling flow in a straight pipe, J. Fluid Mech., 225, 445-479, (1991).

[20] F. Chang and V. K. Dhir, Turbulent flow field in tangentially injected swirl flows in tubes, Int. J. Heat Fluid Flow, 15, 346–356 (1994).

[21] F. Chang and V. K. Dhir, Mechanisms of heat transfer enhancement and slow decay of swirl in tubes using tangential injection, Int. J. Heat Fluid Flow, 16, 78–87 (1995).

[22] M. Yilmaz, O. Comakli and S. Yapici, Enhancement of heat transfer by turbulent decaying swirl flow, Energy Convers. Manage., 40, 1365-1376 (1999).

[23] M. Yilmaz, O. Comakli, S. Yapici and O. N. Sara, Heat transfer and friction characteristics in decaying swirl flow generated by different radial guide vane swirl generators, Energy Convers. Manage., 44, 283-300 (2003).

[24] R. E. Spall and B. M. Ashby, A numerical study of vortex break down in turbulent swirling flows, Trans ASME J Fluids Eng, 122, 179-183(2000).

[25] A. F. Najafi, M. H. Saidi, M.S. Sadeghipour and M. Souhar, Numerical analysis of turbulent swirling decay pipe flow. Int. Comm. Heat and MassTransfer, 32, 627-638 (2005).

[26] A. F. Najafi, M. H. Saidi, M.S. Sadeghipour and M. Souhar, Numerical investigations on swirl intensity decay rate for turbulent swirling flow in a fixed pipe, Int. J. Mechanical sciences, 53, 801-811 [2011].

[27] A. Durmus, A. Durmus and M. Esen, Investigation of heat transfer and pressure drop in a concentric heat exchanger with snail entrance, Applied Thermal Engineering, 22, 321–332 (2002).
[28] S. Eiamsa-ard, S. Rattanawong and P. Promvonge, Turbulent convection in round tube equipped with propeller type swirl generators, Int. Comm. Heat Mass Transfer, 36, 357-364 (2009).
[29] Irfan Kurtbas, Aydın Durmus, Haydar Eren and Emre Turgut, Effect of propeller type swirl generators on the entropy generation and efficiency of heat exchangers, International Journal of Thermal Sciences, 46, 300–307 (2007).
[30] J. A. Eastman, S. R. Phillpot, S. U. S. Choi and P. K. Keblinski, Thermal transport in nanofluids, Annual Review of Materials Research, 34, 219-246, (2004).
[31] L. G. Asirvatham, B. Raja, D. M. Lal and S. Wongwises, Convective heat transfer of nanofluids with correlations, Particuology, 9, 626-631, (2011).
[32] M. Awais, N. Ullah, J. Ahmad, F. Sikandar, M. M. Ehsan, S. Salehin and A. A. Bhuiyan, Heat transfer and pressure drop performance of Nanofluid: A state-of-the-art review, Int. J. Thermofluids, 9, 100065 (2021).
[33] S. U. S. Choi and J. A. Eastman, Enhancing thermal conductivity of fluids with nanoparticles, in ASME International Mechanical Engineering Congress and Exhibition, San Francisco, CA, USA, (1995).
[34] B. C. Pak and Y. I. Cho, Hydrodynamic and heat transfer study of dispersed fluids with submicron metallic oxide particles, Experimental Heat Transfer, 11, 151-170 (1998).
[35] L. S, Sundar, K. V. Sharma and S. Ramanathan, Experimental investigation of heat transfer enhancements with Al_2O_3 nanofluid and twisted tape insert in a circular tube, International Journal of Nanotechnology and Applications, 1, 21-28 (2007).
[36] G. Murali, B. Nagendra, J. Jaya, CFD analysis on heat transfer and pressure drop characteristics of turbulent flow in a tube fitted with trapezoidal-cut twisted tape insert using Fe_3O_4 nanofluid, Materials Today: Proceedings, 21, 313–319 (2020).
[37] A. M. Hussein, R. Abu bakar, K. Kadirgama and K. V. Sharma, Heat transfer enhancement with elliptical tube under turbulent flow TiO_2-water nanofluid, Thermal Science, 20, 89-97 (2016).
[38] E. I. Jassim and F. Ahmed, Experimental assessment of Al_2O_3 and Cu nanofluids on the performance and heat leak of double pipe heat exchanger, Heat Mass Transfer, 56, 1845-1858 (2020).
[39] M. H. Bahmani, Gh. Sheikhzadeh, M. Zarringhalam, O. A. Akbari, A. Alrashed, Gh. Ahmadi Sh. Shabani, M. Goodarzi, Investigation of turbulent heat transfer and nanofluid flow in a double pipe heat exchanger, Advanced Powder Technology, 29, 273-282 (2018).
[40] W. Duangthongsuk and S. Wongwises, Heat transfer enhancement and pressure drop characteristics of TiO_2–water nanofluid in a double-tube counter flow heat exchanger, Int. J. Heat Mass Transfer, 52, 2059-2067 (2009).
[41] W. Duangthongsuk and S. Wongwises, An experimental study on the heat transfer performance and pressure drop of TiO_2-water nanofluids flowing under a turbulent flow regime, Int. J. Heat Mass Transfer, 53, 334-344 (2010).
[42] A. A. Gkountas, L. Th. Benos, G. N. Sofiadis and I. E. Sarris, A printed-circuit heat exchanger consideration by exploiting an Al_2O_3-water nanofluid: Effect of the nanoparticles interfacial layer on heat transfer, Thermal Science and Engineering Progress, 22, 100818 (2021).
[43] FLUENT 15 theory guide, ANSYS Inc., 2013.
[44] K. V. Sharma, P. K. Sarma, W. H. Azmi, R. Mamat and K. Kadirgama, Correlations to predict friction and forced convection heat transfer coefficients of water based nanofluids for turbulent flow in a tube, Int. J. Microscale and Nanoscale Thermal and Fluid Transport Phenomena (IJMNTFTP), 3, 1-25 (2012).
[45] S.E. Kim and D. Choudhury, A Near-Wall Treatment Using Wall Functions Sensitized to Pressure Gradient, In ASME FED Vol. 217, Separated and Complex Flows. ASME. (1995).
[46] F. P. Incropera and D. P. Dewitt, Fundamentals of Heat and Mass Transfer. USA: John Wiley& Sons, Inc., (1996).